



**UNIVERSIDADE ESTADUAL DE CAMPINAS  
SISTEMA DE BIBLIOTECAS DA UNICAMP  
REPOSITÓRIO DA PRODUÇÃO CIENTÍFICA E INTELECTUAL DA UNICAMP**

**Versão do arquivo anexado / Version of attached file:**

Versão do Editor / Published Version

**Mais informações no site da editora / Further information on publisher's website:**

<https://www.sciencedirect.com/science/article/pii/S0008622318306882>

**DOI: 10.1016/j.carbon.2018.07.038**

**Direitos autorais / Publisher's copyright statement:**

©2018 by Pergamon Press. All rights reserved.

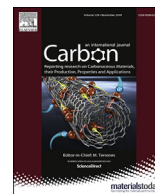
DIRETORIA DE TRATAMENTO DA INFORMAÇÃO

Cidade Universitária Zeferino Vaz Barão Geraldo

CEP 13083-970 – Campinas SP

Fone: (19) 3521-6493

<http://www.repositorio.unicamp.br>



# On the mechanical properties of novamene: A fully atomistic molecular dynamics and DFT investigation

Eliezer Fernando Oliveira<sup>a, b</sup>, Pedro Alves da Silva Autreto<sup>a, c</sup>,  
Cristiano Francisco Woellner<sup>a, b, d</sup>, Douglas Soares Galvao<sup>a, b, \*</sup>

<sup>a</sup> Group of Organic Solids and New Materials (GSONM), Gleb Wataghin Institute of Physics, University of Campinas (UNICAMP), Campinas, SP, Brazil

<sup>b</sup> Center for Computational Engineering & Sciences (CCES), University of Campinas - UNICAMP, Campinas, SP, Brazil

<sup>c</sup> Center of Natural Human Science, Federal University of ABC (UFABC), Santo Andre, SP, Brazil

<sup>d</sup> Physics Department, Federal University of Paraná (UFPR), Curitiba, PR, Brazil

## ARTICLE INFO

### Article history:

Received 21 April 2018

Received in revised form

18 July 2018

Accepted 19 July 2018

Available online 20 July 2018

### Keywords:

Carbon allotrope

Mechanical properties

Molecular dynamics simulation

Novamene

## ABSTRACT

We have investigated through fully atomistic reactive molecular dynamics and density functional theory simulations, the mechanical properties and fracture dynamics of single-ringed novamene (1R-novamene), a new 3D carbon allotrope structure recently proposed. Our results showed that 1R-novamene is an anisotropic structure with relation to tensile deformation. Although 1R-novamene shares some mechanical features with other carbon allotropes, it also exhibits distinct ones, such as, extensive structural reconstructions. 1R-novamene presents ultimate strength ( $\sim 100$  GPa) values lower than other carbon allotropes, but it has the highest ultimate strain along the z-direction ( $\sim 22.5\%$ ). Although the Young's modulus ( $\sim 600$  GPa) and ultimate strength values are smaller than for other carbon allotropes, they still outperform other materials, such as for example silicon, steel or titanium alloys. With relation to the fracture dynamics, 1R-novamene is again anisotropic with the fracture/crack propagation originating from deformed heptagons and pentagons for x and y directions and broken  $sp^3$  bonds connecting structural planes. Another interesting feature is the formation of multiple and long carbon linear chains in the final fracture stages.

© 2018 Elsevier Ltd. All rights reserved.

## 1. Introduction

During the last decades, carbon-based structures have been one of the active areas in material science research. This is due in part to the versatility of carbon atom hybridization ( $sp$ ,  $sp^2$ , and  $sp^3$ ), which can produce a plethora of possible materials with equal diversity on mechanical, thermal and electronic properties [1,2].

Using only one hybridization type, it is possible to produce allotropes with different topologies and dimensionalities, such as fullerenes (0D), carbon nanotubes (1D), graphene (2D), graphite (3D), and diamond (3D). The mix of different hybridizations in the same structure increases this number of possibilities substantially, and using this approach it is possible to generate 2D and 3D new allotrope structures [3–9].

Some of these proposed structures are based on mixing  $sp^2$  regions (graphene-like) with  $sp^3$  ones (diamond-like) in the same material. One example is a series of ultrastrong (two times than usual ceramics), hard and exceptionally lightweight carbons recently produced by compressing  $sp^2$  hybridized glassy carbon at several temperatures [10]. These structures are formed by a local buckling in graphene membranes using  $sp^3$  nodes, which results in an interpenetrating graphene network with long-range order. Those structures have also exceptional compressive strengths with elastic recovery after local deformations. This type of carbon-based structure is an optimal ultralight, ultra strong material for a wide range of multifunctional applications, and the synthesis methodology demonstrates potential to access entirely new metastable materials with exceptional properties [11].

Another example within these proposed 3D carbon allotropes, is the family of the so-called novamene structures [6]. They were recently proposed by L. A. Burchfield et al. [6]. They have a 3D structure composed of a combination of hexagonal diamond [12,13] ( $sp^3$  hybridization called lonsdaleite) and hexagonal carbon rings

\* Corresponding author. Group of Organic Solids and New Materials (GSONM), Gleb Wataghin Institute of Physics, University of Campinas (UNICAMP), Campinas, SP, Brazil.

E-mail address: [galvao@ifi.unicamp.br](mailto:galvao@ifi.unicamp.br) (D.S. Galvao).

( $sp^2$  hybridization) [14,15] (see Fig. 1). The number of hexagonal carbon rings determines the structure type in the family, such as, single-ringed novamene, double-ringed novamene, triple-ringed novamene, and so on [6]. From a topological point of view, novamene can be also considered as a hexagonal diamond structure ( $sp^3$ ) “doped” by carbon hexagons ( $sp^2$ ). First-principles simulations have shown that the single-ringed novamene (Fig. 1(a)), presents an electronic indirect bandgap of  $\sim 0.3$  eV and could be an excellent candidate to be used in electronic devices, such as integrated circuits, optoelectronics, Hall effect sensors, among others [1,2,6]. These complex topologies of mixing of  $sp^2$  and  $sp^3$  can also result in interesting mechanical properties, but they have not been yet investigated to novamenes and it is one of the objectives of the present work.

We investigated the electronic and mechanical properties of single-ringed novamene (1R-novamene) family member through first principles (DFT) and fully atomistic reactive molecular dynamics calculations. Besides determining the elastic properties, we have also investigated the fracture mechanisms of the structures in tensile/elongation regimes.

## 2. Materials and methods

We present in Fig. 1(a) the geometrical structure of 1R-novamene, accordingly to the proposed model by L. A. Burchfield et al. [6]: a hexagonal crystalline arrangement, with a unit cell size (inset I) of  $a_0 = b_0 = 8.40$  Å and  $c_0 = 4.99$  Å (52 carbon atoms) with lattice angles of  $\alpha = \beta = 90^\circ$  and  $\gamma = 120^\circ$ . The carbon atoms are colored differently by regions, in order to help to better visualize the material topology (Fig. 1(a) - inset II). The violet colored areas are

related to an atomic arrangement formed by  $sp^2$  bonds, which are connected to three carbon atom pentagons, in blue. The yellow and the green regions are non-planar hexagons and heptagons, respectively, that are connected by  $sp^3$  bonds. The orange areas are related to the external hexagons that form a plane, which are below of the red atoms.

From a tridimensional point of view, 1R-novamene can be considered as an ABA'B' packing along the z-direction (Fig. 1(b)). The BB' planes are connected in regions without pentagons by a set of carbons (purple in Fig. 1(a) - inset III and Fig. 1(b)). Such atoms can be “switched” between B and B' planes ( $sp^3$  to  $sp^2$  hybridization and vice-versa). By “switching” atoms we meant atoms that can alternately connect up and down BB' planes (see details in Ref. [6]).

The molecular dynamics (MD) simulations were carried out using the ReaxFF force field [16], as implemented in the computational code Large-scale Atomic/Molecular Massively Parallel Simulator (LAMMPS) [17]. Periodic boundary condition (PBC) was used. The considered hexagonal supercell size was  $5a_0 \times 5b_0 \times 5c_0$  (6500 atoms) with lattice angles of  $\alpha = \beta = 90^\circ$  and  $\gamma = 120^\circ$ , which is large enough to avoid spurious size effects (such as, contributions of low energy/long wavelength oscillations) [18]. The initial 1R-novamene geometry was energetically minimized using conjugate gradient technique, and then followed by a thermal equilibration at room temperature (300 K) in an NPT ensemble at the constant hydrostatic pressure of 0 GPa. We observed in this step that 1R-novamene structure is stable and the supercell size does not change significantly. After the system thermal equilibration, a uniaxial tensile strain rate of  $10^{-6}$  fs $^{-1}$  (up to 50%) was applied to deform the structure. This strain rate has been applied with success for mechanical properties studies in other carbon nanostructures as

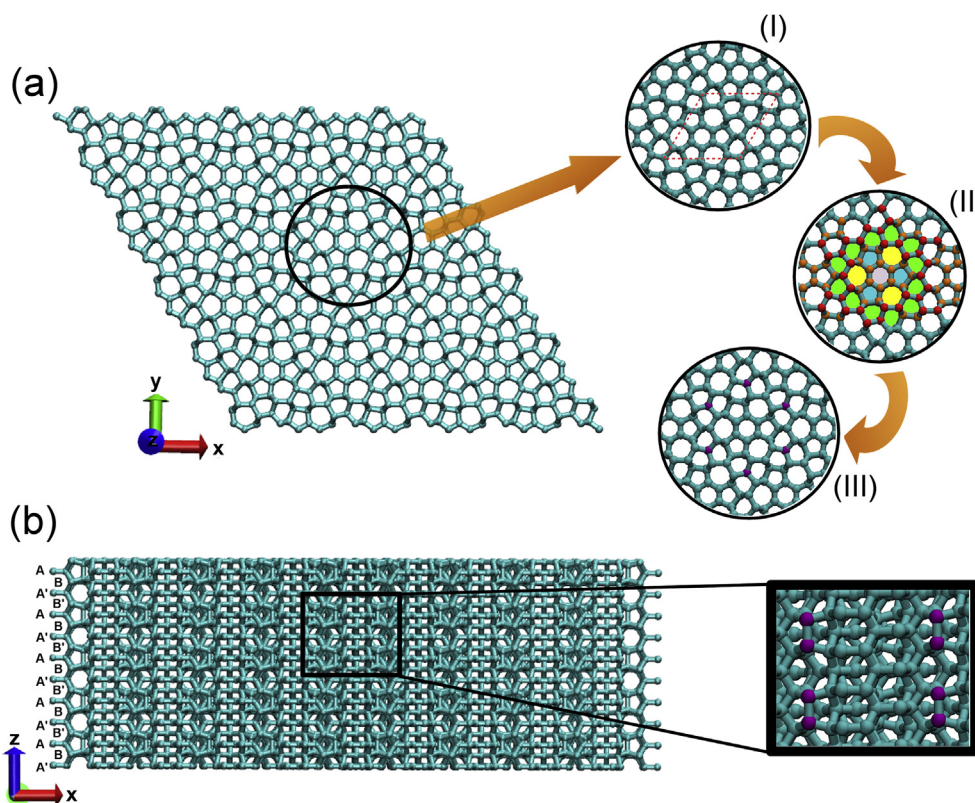


**Fig. 1.** Geometrical structure of a single-ringed novamene supercell. (a) Top of view: (I) top representation of a unit cell; (II) orange and red atoms belong to different planes and the arrangement of the carbon atoms form hexagons (in violet), pentagons (in blue), distorted heptagons (in yellow), and distorted hexagons (in green); (III) “switching” atoms that can alternately connect two BB' stacking layers (see part (b)). (b) Lateral view represents the ABA'B' layer stacking; the inset shows how the “switching” atoms connect BB' planes. (A colour version of this figure can be viewed online.)

diamond, nanotubes, graphene, and others [19]. The stress-strain behavior was calculated by strain applied along cartesian x, y, and z-directions (orthogonal system shown in Fig. 1); this will give the normal stresses  $\sigma_x$ ,  $\sigma_y$ , and  $\sigma_z$ . During the uniaxial tensile procedure, a NPT ensemble was used to keep the system temperature at 300 K and an external pressure of 0 GPa for the perpendicular and shear directions of the tensile one. It is important to use this procedure in order to avoid undesired stresses that can affect the final results during the tensile procedure. We also calculated the second invariant of the deviatoric stress tensor, the von Mises stress [20] for each atom during the straining process. The von Mises yield criterion suggests that fracture starts when this stress value reaches the yield strength of the material [20]. For all MD runs, a timestep of 0.25 fs was considered. This general stress-strain procedure, time-step, and strain rate adopted here were already proved to be effective to study the mechanical properties of carbon nanostructures [19].

Due to the large size of the unit cell, the complete strain-stress and fracture analyses using *ab initio* methods is cost-prohibitive, but obtaining the elastic constant and band structure for static calculations is feasible. Also, it is well-known that although fracture dynamics is well described by ReaxFF, it tends to underestimates

the elastic constants [19,21], thus the use of *ab initio* methods will provide a better estimate of these values.

Our first principles calculations were performed using CASTEP code [22], a plane-wave implementation of density functional theory (DFT). The exchange-correlation (XC) contribution to the DFT energy was calculated using the GGA/PBE functional [23]. For comparison purposes, we also calculated the structure using LDA/CAPZ functional [24]. Convergence criteria employed for both the electronic self-consistent relaxation and the ionic relaxation were set to 10 eV and 0.006 eV/Å for energy and force, respectively.

### 3. Results and discussions

In Fig. 2(a) we present the stress-strain curves for 1R-novamene under tensile deformation along x, y, and z-directions (see Fig. 1). Our results indicate a significant anisotropic behavior, quite distinct from the ones reported to graphene and diamond [25–30]. The abrupt drop of the stress values (ultimate strength) without a clear plastic region also indicates a brittle material. It should be stressed that although the x and y stress-strain curves are similar (in-plane strain), their deformation mechanisms (involving pentagons and/or hexagons) are different (inset of Fig. 2(a)), which results in a slightly

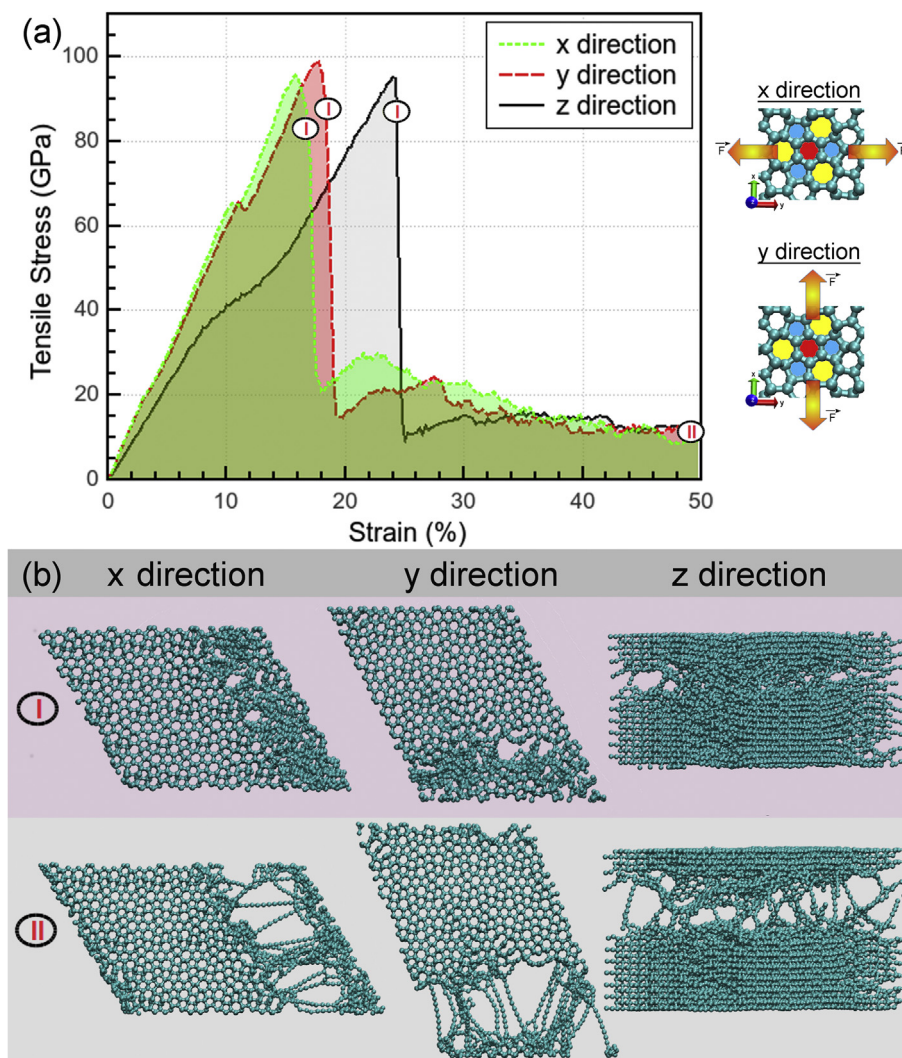


**Fig. 2.** (a) Stress-strain curves for tensile deformation along x, y, and z 1R-novamene directions; the inset highlights that x and y deformations are not equivalent; (b) MD snapshots of two deformation stages for each tensile direction: (I) structure just after the structural failure/fracture and; (II) structure at 50% strain. (A colour version of this figure can be viewed online.)



different ultimate strength (95.6 and 98.7 to x and y-directions, respectively). This chirality-dependent deformation mechanism is similar to what was reported for silicene [31] and chalcogenides [32].

For the z-direction (inter-plane strain), the 1R-novamene deformation is more pronounced and reaches the ultimate strain at a higher value than the corresponding ones for x and y directions (24.5% in comparison to 15.5% and 17.5%, respectively). Some representative MD snapshots are presented in Fig. 2(b). It is possible to observe that despite the brittle behavior, multiple linear carbon chains (linear atomic chains, LAC) are formed. Although the LAC in 1R-novamene is not yet reported, LAC has been theoretically predicted and observed experimentally in other carbon-based nanostructures [33–38].

In Fig. 3(a) we present the percentage amount of pure  $sp^2$ ,  $sp^3$ , and broken bonds during the tensile elongation along the x-direction. These percentages are related to the total number of initial bonds in 1R-novamene before the tensile process (9759 bonds, in which around 66% of them were  $sp^3$  and 34% were  $sp^2$ ). Knowing that the expected bond length for the  $sp$ ,  $sp^2$  or  $sp^3$  are, respectively,  $\sim 1.37$  Å,  $\sim 1.47$  Å, and  $\sim 1.54$  Å, we evaluate the bond length between

carbon atoms, counting which one have its bond length close to a  $sp$ ,  $sp^2$  or  $sp^3$  values, with a tolerance of  $\pm 0.04$  Å from the bond expected value. During the tensile process, the distances between carbon atoms that become above to the  $sp^3$  bond length was considered non-bonded and computed as broken bonds. Some representative MD snapshots are shown in Fig. 3(b). As we can see, when 1R-novamene is stretched along the x-direction, the number of  $sp^2$  and  $sp^3$  carbon bonds decreases, while the number of broken bonds increases, as expected. The deformation behavior is almost linear up to  $\sim 10\%$ , when it is observed a slight drop in the stress/strain curve (Fig. 2(a)). A detailed analysis of this region (between 10.5% and 10.7%) showed that the number of  $sp^2$ ,  $sp^3$ , and broken bonds remain practically constant (see inset of Fig. 3(a)), which is suggestive that the 1R-novamene undergoes structural rearrangements, without the formation and/or breaking of covalent bonds. After this stage, the stress increases as well as the number of newly formed  $sp^2$  bonds (from the heptagons), up to reaching a plateau that remains almost constant up to reaching the structural failure. After fracture, there is still a partial 'healing' with the formation of new chemical bonds, mainly in  $sp^2$  hybridization form. Such results are corroborated by the pair radial function  $g(r)$  presented in Fig. S1, in supplementary material. During the tensile process (independent whether it is performed along x, y, or z directions),  $sp$  bonds are also formed, but in a small number (at most 3%). This is an indicative that the bonds in 1R-novamene are dominated by  $sp^2$  and  $sp^3$  ones. Based on this, we did not present the  $sp$  bonds curve in Fig. 3.

From the MD snapshots (Fig. 3(b)), we can see that bond breaking occurs along the applied tensile direction, as expected (highlighted in red in Fig. 3(b)). The 1R-novamene fracture produces multiple LAC, as evidenced in Fig. 3(b) for strain at 48%. This formation suggests that some of the broken bonds can also form  $sp$ - $sp^2$ ,  $sp$ - $sp^3$ , or  $sp$ - $sp$  bonds. A similar behavior was observed for y-direction (see Figs. S2 and S3 in SM).

For the z-direction the process is significantly different (Fig. 3(c)). 10% strain is enough to increase the number of  $sp^2$  bonds in relation to  $sp^3$  ones (see also the corresponding  $g(r)$  - Fig. S4). This  $sp^2$  to  $sp^3$  conversion keeps the number of broken bonds constant after increasing almost linearly. This conversion can continue up to the fracture limit (24.5%). The representative MD snapshots in Fig. 3(d) show that the number of  $sp^2$  bonds during the tensile elongation is closed related to the number "switching" carbon atoms along the z-direction. In the absence of applied strain, the "switching" carbon atoms are connected by  $sp^3$  bonds. When the strain reaches values around 11%, the bonds related to the "switching atoms" become highly stretched and eventually breaks. At this moment, these bonds change to  $sp^2$ -type, as seen in the snapshot for 16% of strain (Fig. 3(d)). As consequence, the number of  $sp^3$  bonds decreases, while the  $sp^2$  ones increase. It is interesting to note that this  $sp^3$  to  $sp^2$  bonds conversion occurred in the "switching" carbon atoms during the tensile elongation in z-direction could cause a dramatic change in the electronic structure of the 1R-novamene. According to L. A. Burchfield et al. [6], the stable 1R-novamene is a semiconductor, but when the "switching" carbon atoms are in a  $sp^2$  configuration, a metal-like behavior will appear. Then, stretching the 1R-novamene in the z-direction will eventually cause a semiconductor to metal transition. After fracture, multiple LAC are also present (see the snapshot for 48% of strain in Fig. 3(d)). As we can see from Fig. 3, in contrast to graphene, diamond and carbon nanotubes, 1R-novamene presents a structural reconstruction after the crack opening after the sudden stress change, with an increase of the covalent bonds ( $sp^2$  and  $sp^3$ ).

In Fig. 4 we present MD representative snapshots of the tensile procedure with atoms colored accordingly to von Mises stress values. The complete deformation processes are presented in the supplementary videos (Videos S1, S2, and S3). As can be seen from

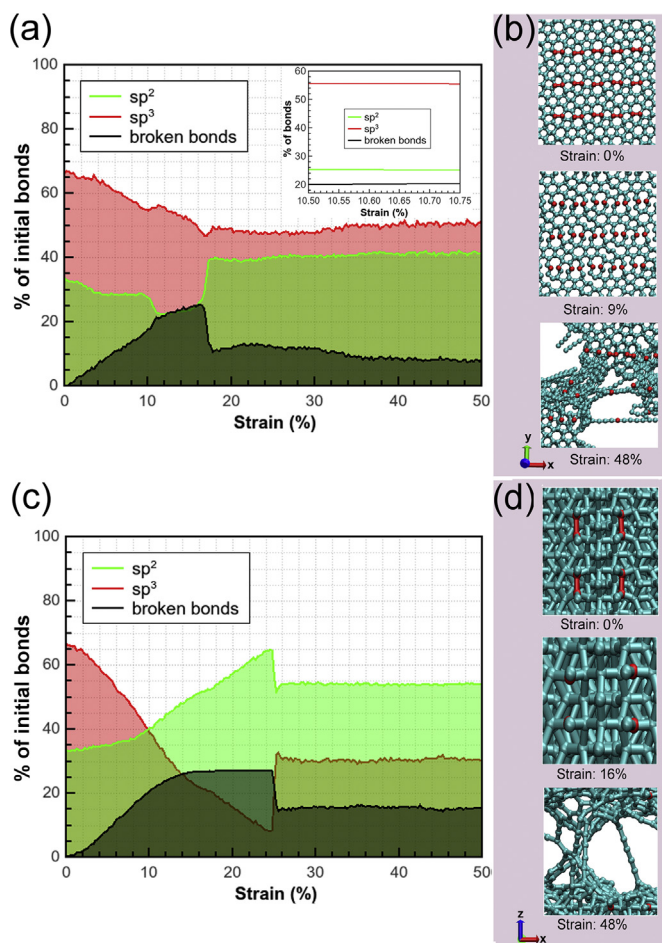


**Fig. 3.** Percentage of the number of  $sp^2$ ,  $sp^3$ , and broken bonds during the tensile testing: (a) x-direction with some of its (b) representative MD snapshots at some strain levels, and (c) z-direction with some of its (d) representative MD snapshots for some strain levels. The atoms highlighted in red in the parts (b) and (d) represent some atoms in which their bonds will break during the tensile testing along the x and z-direction, respectively. The bonds percentages were obtained about the total number of bonds in the 1R-novamene, before the tensile process begins (9759 bonds, in which around 66% of them were  $sp^3$ , and 34% were  $sp^2$ ). (A colour version of this figure can be viewed online.)

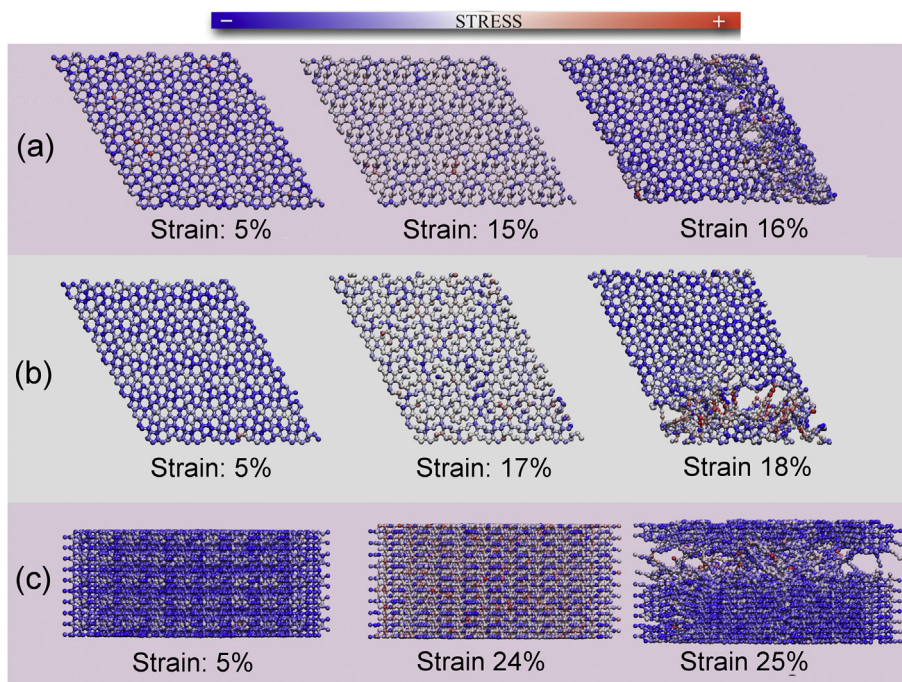


**Fig. 4.** Stress accumulation during the tensile elongation along: (a) x, (b) y, and; (c) z-directions for some selected strain values: middle of the first linear regime and stages before and after the 1R-novamene mechanical failure/fracture. The colors represent the stress levels (from low (blue) to high (red) ones). (A colour version of this figure can be viewed online.)

**Table 1**  
Mechanical properties obtained with ReaxFF force field for 1R-novamene (this work) and some selected carbon allotropes [19] at 300 K; the available experimental data [25–30,39] are presented into parentheses.

Structure	Ultimate Strength (GPa)	Ultimate Strain (%)	Young's Modulus (GPa)	Poisson's Ratio $\sigma_{ij}$
1R-novamene (x) (this work)	95.6	14.7	674.2	$\sigma_{yx} = 0.60$
1R-novamene (y) (this work)	98.7	16.3	659.7	$\sigma_{zx} = 0.04$
1R-novamene (z) (this work)	95.2	22.5	438.8	$\sigma_{xy} = 0.60$
Diamond (z)	148.7 (86–100)	18.9 (12.0)	1300.0 (1188.0)	$\sigma_{zy} = 0.04$
Graphene (armchair)	149.6 (130.0)	21.5 (25.0)	1266.0 (1000.0)	$\sigma_{xz} = 0.50$
Nanotube (12,0)	111.3 (20–50)	21.6 (1–6)	1214.0 (320–1470)	$\sigma_{yz} = 0.50$
				$\sigma_{zx} = 0.04$ (0.07)
				$\sigma_{yz} = 0.04$ (0.04)
				0.91 (–0.19)
				–

**Fig. 4.** for x and y-directions, the stress per atom is initially well-distributed and concentrated mainly on the carbon atoms belonging to non-planar heptagons and hexagons. The fracture/crack propagation originated from these regions and the atoms composing the LAC came from broken heptagons and pentagons rings (see Videos S1 and S2).

Supplementary video related to this article can be found at <https://doi.org/10.1016/j.carbon.2018.07.038>.

In the case of z-direction, the stress is initially concentrated on the carbon atoms in  $sp^3$  hybridization (including the “switching” carbon atoms), perpendicular to the tensile direction. Those regions will be the ones where the bonds will be broken. As the stress accumulates in the  $sp^3$  bonds, it will deform the heptagons, and these deformations originate the fracture/crack propagation (see video S3). The remaining bonded atoms from the non-planar heptagons and hexagons also form the carbon lines as the 1R-novamene stretching continues. So, in general, the cracks in 1R-novamene come from the non-planar heptagons, hexagons and planar pentagons stretching during the tensile process.

In Table 1 we compare some mechanical properties calculated to

1R-novamene with other carbon nanostructures. The ultimate strength and strain, Young's modulus, and Poisson's ratio for graphene (armchair), carbon nanotube (12,0) and cubic diamond calculated using the same ReaxFF force field [19] are displayed in Table 1. We also present the experimental data obtained from Refs. [25–30,39]. Our results show that 1R-novamene has an ultimate strength smaller than the other carbon allotropes. Regarding the ultimate strain, 1R-novamene along the z-direction has the highest one, which means it can stand larger deformations before fracture in comparison to the other listed carbon allotropes.

As mentioned before from the stress-strain analyses, 1R-novamene is an anisotropic material, thus different Young's modulus (E) values are expected depending on deformation direction, as confirmed in Table 1. Young's modulus values are smaller than the others carbon allotropes considered here, which suggests that 1R-novamene is easier to deform, which is consistent with the Poisson's ratio values presented in Table 1 ( $\sigma_{ij}$ , where the  $j$  represents the tensile direction and  $i$  a perpendicular direction to the tensile one [40]). Although Young's modulus and ultimate strength values are smaller than for the other structures listed in Table 1, they still

outperform other materials, such as silicon, steel or titanium alloys [39].

To compare the trends of elastic constant values, we also carried out DFT calculations using the functionals GGA/PBE and LDA/CAPZ, as discussed in the Materials and Methods section. We first optimized the 1R-novamente unit cell, and then we calculated the energy band structure, as shown in Fig. S5 of the SM. The calculations show the structure is a semiconductor and has an indirect band gap equals 0.440 eV with GGA/PBE and 0.420 eV with LDA/CAPZ. These values are quite similar to the value 0.335 eV reported by L. A. Burchfield et al. [6]. We then calculated Young's modulus and Poisson's ratio values for the optimized structure. Although the DFT (see Table S1 of the SM) and ReaxFF values are different, as expected, the general trends are consistent.

#### 4. Summary and conclusions

We have investigated through fully atomistic reactive (ReaxFF potential) molecular dynamics and DFT (GGA/PBE and LDA/CAPZ functionals) simulations, the mechanical properties and fracture dynamics of a newly proposed carbon allotrope, named novamene. Novamene is a 3D structure composed of hexagonal diamond ( $sp^3$  hybridization called lonsdaleite) and hexagonal carbon rings ( $sp^2$  hybridization). In the present work we considered the single-ringed novamene (1R-novamene) structure.

Our results showed that 1R-novamene is an anisotropic structure with relation to tensile deformation, presenting similar behavior for x and y directions, but a distinct one for the z direction. Although 1R-novamente shares some mechanical features with other carbon allotropes, such as a brittle fracture behavior (diamond) and the formation of multiple carbon linear chains in the final fracture stages (graphene), it also exhibits distinct ones, such as, an extensive structural reconstruction.

Our simulation estimates a 1R-novamene ultimate strength (~100 GPa) lower than other carbon allotropes but has the highest ultimate strain along the z-direction (~22.5%), which means it can stand larger deformations before fracture. Although the calculated Young's modulus (~600 GPa) and ultimate strength values are smaller than for other carbon allotropes, they still outperform other materials, such as for example silicon, steel or titanium alloys.

With relation to the fracture dynamics, 1R-novamene is again anisotropic. While for the x and y directions the fracture/crack propagation originates from deformed heptagons and pentagons, for the z directions is mainly related to broken  $sp^3$  bonds connecting structural planes. Another interesting feature is the formation of multiple and long carbon linear chains in the final fracture stages.

Further studies should be carried out to better characterize the 1R-novamene properties, as for example electrical and thermal transport, which could better determine its potential technological applications. Also, it will be interesting to investigate other types of novamene structures (double-ringed, triple-ringed, etc) in order to determine how the amount of initial  $sp^2$  bonds (related to the number of carbon hexagons) into the hexagonal diamond structure will affect the mechanical properties of the resulting material. It was recently demonstrated for Schwarzites (another class of negative curvature carbon allotrope) [41], that the ratio of different structural rings (pentagons, hexagons, etc.) are of fundamental importance to determine the material response to tensile and/or compression deformation. We hope the present study will stimulate further studies along these lines.

#### Acknowledgments

We would like to thank the Brazilian agency FAPESP (Grants

2013/08293–7, 2014/24547–1 and 2016/18499–0) for financial support. Computational and financial support from the Center for Computational Engineering and Sciences at Unicamp through the FAPESP/CEPID Grant No. 2013/08293–7 is also acknowledged. Support from the Brazilian Agencies CNPq and CAPES is also acknowledged.

#### Appendix A. Supplementary data

Supplementary data related to this article can be found at <https://doi.org/10.1016/j.carbon.2018.07.038>.

#### References

- [1] T.D. Burchell, Carbon Materials for Advanced Technologies, first ed., Elsevier Science, Oxford, 1999.
- [2] G. Messina, S. Santangelo, Carbon: the Future Material for Advanced Technology Applications, first ed., Springer, New York, 2006.
- [3] J. Narayan, A. Bhaumik, Novel phase of carbon, ferromagnetism, and conversion into diamond, *J. Appl. Phys.* 118 (2015) 215303.
- [4] C. He, L. Sun, C. Zhang, J. Zhong, Two viable three-dimensional carbon semiconductors with an entirely  $sp^2$  configuration, *Phys. Chem. Chem. Phys.* 15 (2) (2013) 680–684.
- [5] X.-L. Sheng, Q.-B. Yan, F. Ye, Q.-R. Zheng, G. Su, T-Carbon: a novel carbon allotrope, *Phys. Rev. Lett.* 106 (2011) 155703.
- [6] L.A. Burchfield, M.A. Fahim, R.S. Wittman, F. Delodovici, N. Manini, Novamene: a new class of carbon allotropes, *Heliyon* (2) (2017) 3, e00242.
- [7] N.V.R. Nulakani, V. Subramanian, Cp-Graphyne: a low-energy graphyne polymorph with double distorted Dirac points, *ACS Omega* 2 (10) (2017) 6822–6830.
- [8] F. Delodovici, N. Manini, R.S. Wittman, D.S. Choi, M.A. Fahim, L.A. Burchfield, Protomene: a new carbon allotrope, *Carbon* 126 (2018) 547–579.
- [9] X. Wang, J. Rong, Y. Song, X. Yu, Z. Zhan, J. Deng, QPHT-graphene: a new two-dimensional metallic carbon allotrope, *Phys. Lett. A* 381 (34) (2017) 2845–2849.
- [10] M. Hu, J. He, Z. Zhao, T.A. Strobel, W. Hu, D. Yu, et al., Compressed glassy carbon: an ultrastrong and elastic interpenetrating graphene network, *Sci. Adv.* 3 (6) (2017) e1603213.
- [11] S. Vinod, C.S. Tiwary, P.A.S. Autreto, J. Taha-Tijerina, S. Ozden, A.C. Chipara, et al., Low-density three-dimensional foam using self-reinforced hybrid two-dimensional atomic layers, *Nat. Commun.* 5 (2014) 4541.
- [12] C. Frondel, U.B. Marvin, Lonsdaleite, a hexagonal polymorph of diamond, *Nature* 214 (1967) 587–589.
- [13] F.P. Bundy, J.S. Kasper, Hexagonal Diamond—a new form of carbon, *J. Chem. Phys.* 46 (1967) 3437.
- [14] P.Y. Bruice, Organic Chemistry, third ed., Pearson, New Jersey, 2001.
- [15] J.E. McMurry, Organic Chemistry, 7rd ed., Thomson Learning, Belmont, 2008.
- [16] A.C.T. van Duin, S. Dasgupta, F. Lorant, W.A. Goddard, ReaxFF: A reactive force field for hydrocarbons, *J. Phys. Chem. A* 105 (41) (2001) 9396–9409.
- [17] S.J. Plimpton, Fast parallel algorithms for short-range molecular dynamics, *Comput. Phys.* 117 (1) (1995) 1–19.
- [18] D. Frenkel, B. Smit, Understanding Molecular Simulation: from Algorithms to Applications, second ed., Academic Press, San Diego, 2001.
- [19] B.D. Jensen, K.E. Wise, G.M. Odegard, The effect of time step, thermostat, and strain rate on ReaxFF simulations of mechanical failure in diamond, graphene, and carbon nanotube, *J. Comput. Chem.* 36 (21) (2015) 1587–1596.
- [20] A. Zang, O. Stephansson, Stress Field of the Earth's Crust, first ed., Springer, Houten, 2009.
- [21] B.D. Jensen, K.E. Wise, G.M. Odegard, Simulation of the elastic and ultimate tensile properties of diamond, graphene, carbon nanotubes, and amorphous carbon using a revised ReaxFF parametrization, *J. Phys. Chem. A* 119 (37) (2015) 9710–9721.
- [22] S.J. Clark, M.D. Segall, C.J. Pickard, P.J. Hasnip, M.I.J. Probert, K. Refson, et al., First principles methods using CASTEP, *Kristallogr. Cryst. Mater* 220 (5–6) (2005) 567–570.
- [23] J.P. Perdew, K. Burke, M. Ernzerhof, Generalized gradient approximation made simple, *Phys. Rev. Lett.* 77 (1996) 3865–3868.
- [24] J.P. Perdew, A. Zunger, Self-interaction correction to density-functional approximations for many-electron systems, *Phys. Rev. B* 23 (1981) 5048.
- [25] T. Schneider, E. Stoll, Molecular-dynamics study of a three-dimensional one-component model for distortive phase transitions, *Phys. Rev. B* 1302 (1978) 17.
- [26] H.J. McSkimin, W.L. Bond, Elastic moduli of diamond, *Phys. Rev.* 105 (1957) 116.
- [27] J.E. Field, C.S.J. Pickles, Strength, fracture and friction properties of diamond, *Diamond Relat. Mater.* 5 (6–8) (1996) 625–634.
- [28] R.H. Telling, C.J. Pickard, M.C. Payne, J.E. Field, Theoretical strength and cleavage of diamond, *Phys. Rev. Lett.* 84 (2000) 5160.
- [29] C. Lee, X. Wei, J.W. Kysar, J. Hone, Measurement of the elastic properties and intrinsic strength of monolayer graphene, *Science* 321 (5887) (2008)



- 385–388.
- [30] F. Liu, P. Ming, J. Li, *Ab initio* calculation of ideal strength and phonon instability of graphene under tension, *Phys. Rev. B* 76 (2007) 064120.
- [31] T. Botari, E. Perim, P.A.S. Autreto, A.C.T. van Duin, R. Paupitz, D.S. Galvao, Mechanical properties and fracture dynamics of silicene membranes, *Phys. Chem. Chem. Phys.* 16 (36) (2014) 19417–19423.
- [32] P. Manimunda, Y. Nakanishi, Y.M. Jaques, S. Susarla, C.F. Woellner, S. Bhowmick, et al., Nanoscale deformation and friction characteristics of atomically thin WSe<sub>2</sub> and heterostructure using nanoscratch and Raman spectroscopy, *2D Mater.* 4 (4) (2017), 045005.
- [33] N.F. Andrade, A.L. Aguiar, Y.A. Kim, M. Endo, P.T.C. Freire, G. Brunetto, et al., Linear carbon chains under high-pressure conditions, *J. Phys. Chem. C* 119 (19) (2015) 10669–10676.
- [34] C. Jin, H. Lan, L. Peng, K. Suenaga, S. Iijima, Deriving carbon atomic chains from graphene, *Phys. Rev. Lett.* 102 (2009) 205501.
- [35] A. Chuvilin, J.C. Meyer, G. Algara-Siller, U. LKaiser, From graphene constrictions to single carbon chains, *N. J. Phys.* 11 (2009) 083019.
- [36] G. Moras, L. Pastewka, P. Gumbsch, M. Moseler, Formation and oxidation of linear carbon chains and their role in the wear of carbon materials, *Tribol. Lett.* 44 (2011) 355–365.
- [37] C. Ataca, S. Ciraci, Perpendicular growth of carbon chains on graphene from first-principles, *Phys. Rev. B* 83 (2011) 235417.
- [38] I.E. Castelli, P. Salvestrini, N. Manini, Mechanical properties of carbynes investigated by *ab initio* total-energy calculations, *Phys. Rev. B* 85 (2012) 214110.
- [39] M.F. Yu, B.S. Files, S. Arepalli, R.S. Ruoff, Tensile loading of ropes of single wall carbon nanotubes and their mechanical properties, *Phys. Rev. Lett.* 84 (2000) 5552.
- [40] J.F. Shackelford, *Introduction to Materials Science for Engineers*, sixth ed., Pearson, London, 2015.
- [41] S.M. Sajadi, P.S. Owuor, S. Schara, C.F. Woellner, V. Rodrigues, R. Vajtai, et al., Multiscale geometric design principles applied to 3D printed schwarzites, *Adv. Mater.* 30 (1) (2018) 1704820.